

# Processability of Oriented film for Linear Low Density Polyethylenes

H.Uehara(1)\*, K.Sakauchi(1), T.Kanai(2), T.Yamada(3)

(1) Okura Industrial Co.,Ltd

(2) Idemitsu Petrochemical Co.,Ltd

(3) Kanazawa University

\*Corresponding author : [h-uehara@okr-ind.co.jp](mailto:h-uehara@okr-ind.co.jp)

## Abstract

In the first instance, the relationships between the process conditions and the physical properties of the double bubble tubular film for LLDPE are experimentally studied, in order to proffer theories concerning such relationships. Stretching temperature affects the processability and the properties of stretched film.

In this research, the influence of temperature is studied by using both a double bubble tubular film machine and a laboratory biaxial stretcher.

The influence of shrinkage properties and film physical properties on stretched temperature are studied. In addition the relationship between film shrinkage properties and stretching stress, calculated by measuring the stretching force and the inside bubble pressure during the double bubble tubular film production process are investigated. Finally the relationship between the laboratory biaxial stretching process (tenter type) and the double bubble tubular film process are reported in terms of stretchability.

## 1. Introduction

Double bubble tubular film extrusion is an economic way for producing biaxially oriented film compared to tenter biaxially oriented film. This film manufacturing technique has been widely used to produce biaxially oriented films because of good shrinkage ability and high physical properties.

The double bubble tubular biaxial stretching process has been studied using various resins such as Polyvinylidene Chloride(PVDC), Polyethylene Terephthalate(PET), Polyphenylene Sulfide(PPS), Polyamide(Ny6), Ethylene vinyl alcohol copolymer(EVOH), Polypropylene(PP), Polyethylene(PE).

J.L.White[1] explained the technical trends and typical applications of those resins. Takashige and Kanai[2] reported on the double bubble tubular film process and the theoretical analysis of the stress development and the scaleup rule for Polyamide-6. S.Ree[3] reported on the double bubble tubular film process-processability and the structure development of Polyamide-612. K.Song[4] reported on the processability of the blending of PBT and PET.

The first application of double bubble tubular film extrusion to isotactic polypropylene is attributable to Goldman[5] of Du Pont and is described in his November 6th, 1958 patent application. Since then, many patents[6,7,8,9,10] have been applied for, the double bubble tubular process technology. The double bubble tubular Polypropylene film is mainly used to package stationery, groceries, foods and so on because of comparatively easier processability and relatively cheaper resin cost. But recently, shrinkage film for this usage is required to have a superior appearance and shrinkage strength. The double bubble tubular film of LLDPE has good shrinkage ability and high physical properties. For this reason, the demand for double bubble tubular film of LLDPE has been increasing. Before now, resins patents[11,12,13,14,15] have been applied for.

In general, it is understood that LLDPE has a narrow stretchability range for double bubble tubular film compared with Polypropylene, but until now the stretchability and influence of physical properties on process conditions have not been reported in any detail. This paper will analyze the processability of double bubble tubular film of Linear Low Density Polyethylenes.

## **2. Experimental**

### **2.1 Double bubble tubular machine**

The double bubble tubular film line consists of two stages of bubbles. Figure 1 is a schematic drawing of a double bubble tubular film blowing apparatus. In the first stage, the bubble is blown from a molten state. The first bubble(it is also called the primary tube) is flattened out by a set of nip rolls and re-inflated into a larger second stage bubble at a higher temperature than the materials glass transition temperature. The second bubble is stretched biaxially in the infrared heater oven, and after stretching, the bubble is cooled by air. The second bubble is also flattened out by a set of nip rolls and is slit along both edges, and each film is wound separately. In this report, all double bubble tubular films are produced on an extruder of 65mm diameter with a circular die of 180mm diameter.

### **2.2 Laboratory biaxial stretcher (tenter type )**

Figure 2 is a photograph of the laboratory biaxial stretcher. Square film is set in the center of the machine, and is clipped all around. The film is heated to the appropriate temperature in the set time, and is then stretched biaxially. The stretched film is cooled by air and removed from the machine.

### **2.3 Materials**

The main material studied is Linear Low Density Polyethylene with a density of 0.920 g/cm<sup>3</sup> and a melt flow index of 1.0 g/10min. In order to improve the stretchability, both Linear Low Density Polyethylene with a density of 0.902 g/cm<sup>3</sup> and a melt flow index of 1.0 g/10min and that with a density of 0.935 g/cm<sup>3</sup> and a melt flow index of 2.5 g/10min each are blended as 15% of the total. The effect of blending will be described in the next report. Erucic acid amide is used as slip agent.

## **2.4 Experimental Methods**

### **2.4.1 Double bubble tubular film**

Double bubble tubular film is produced as described in 2.1. The stretch ratio of the machine direction(MD) is 5, and the transverse direction(TD) is 5. The primary tube thickness is 375 µm, and film width is 235mm, while the final stretched film thickness is 15 µm, and film width is 1180mm. The out put rate is 47 kg/h. The stretching torque and inside bubble pressure are influenced by the stretching temperature. The average temperatures measured from 3 zones in the pre-heaters and 3 zones in the stretch heaters, are shown in Table 2. The film temperature after pre-heater is measured by an infrared pyrometer (EDDOX IRT/C.10 made by EXERGEN U.S.A.). The inside bubble pressure is measured by using a pressure gauge (NAGANO KEIKI GC66 made in Japan). This is done by firstly applying a PP tape patch to the surface and making about a 10 mm incision through which the gauge is quickly inserted.

Bubble stretching force is measured by a torque measuring instrument (ONO SOKKI SS201made in Japan) that is set between the pinch roll and driving motor. The stretching force is calculated from the torque.

The necking phenomenon was recorded by digital camera. The bubble deformation behaviour is observed by marking a grid on the pre-stretched film surface. After the marked grid has been stretched, the bubble is stopped and cooled, then wound keeping the shape of the stretched film. The expanded dimensions of the marked grid are measured. The photograph of this bubble is taken after re-inflating, because the stretched area is obstructed by the heater, during the process.

### **2.4.2 Laboratory biaxial stretcher**

The test piece film for laboratory biaxial stretcher is the first bubble film (primary tube) from the double bubble tubular process. The stretch ratio is MD=5 and TD=5. The primary tube thickness is 300 µm, and after stretched film thickness is 12 µm. Film size is a 95mm square and with clip clearance becomes a 70mm square. The stretching speed is 30 mm/sec, and the heating time is 2 minutes.

### 3. Results

#### 3.1 Double bubble tubular film process

The bubble shape in the double bubble tubular film process and also the film properties, are changed by the heating temperatures. So, it is ideal to use the heating temperature as a parameter, however there are many distinct temperature zones before and during stretching. Hence, it is not so easy to use temperatures as a parameter of stretchability. Also the film surface temperatures are difficult to measure because accurate readings are hindered by the infrared heaters. Due to this, the stretching torque is used as a parameter of stretchability, as it shares a close relationship with stretching temperatures. Increasing the stretching temperature, making it easier to stretch, decreases the stretch torque. The stretching torque can be easily measured as it is digitally displayed on the equipment during production. Those stretching torques and the inside bubble pressures during stretching and the stretching stress, which is calculated by torque and inside bubble pressure, and the stretched film properties are shown in table 2. The stretching stress is calculated as follows. The second bubble of double bubble tubular film process is considered as a blown film process as reported by T.Kanai [16,17] and that the force balance on the tubular film is developed from membrane theory. Figure 3 shows a schematic diagram of force balance on the bubble.

Membrane theory leads to a set of forces on the film between positions Z and take up position L. This has the form:

$$F_L = 2\pi RH\sigma_{MD} \cos\theta + \pi(R_L^2 - R^2) \cdot \Delta P \quad (3-1)$$

The stress  $\sigma_{MD}$  and  $\sigma_{TD}$  are related to the pressure  $\Delta P$  through the expression:

$$\frac{H \cdot \sigma_{MD}}{R_1} + \frac{H \cdot \sigma_{TD}}{R_2} = \Delta P \quad (3-2)$$

where  $F_L$  is the bubble tension,  $R$  is the bubble radius,  $R_L$  is the final bubble radius,  $H$  is film thickness,  $\theta$  is the bubble angle, and  $R_1$  and  $R_2$  are appropriate radii of curvature.

$$R_1 = \frac{(1 + (dR/dz)^2)^{3/2}}{(d^2R/dz^2)} \quad (3-3)$$

$$R_2 = \frac{R}{\cos\theta} \quad (3-4)$$

The maximum stretching stresses  $\sigma_{MD}$  and  $\sigma_{TD}$  are closely related to the physical properties of the film. The maximum stress at the final stretching point is used to set up the scale up rule. At the final stretch point, bubble diameter is equal to final diameter.

$$\sigma_{MD\max} = \frac{F_L}{2\pi R_L H_L} \quad (3-5)$$

$$\sigma_{TD\max} = \frac{R_L \cdot \Delta P}{H_L} \quad (3-6)$$

where  $H_L$  is the final film thickness.

This data shows that the double bubble tubular film process is stable within a stretching stress of about 9MPa to 18MPa.

The relationship between the stretching stress and film properties are expressed as figures. The stretching stress and properties are calculated by  $\sqrt{MD \cdot TD}$ .

Figure 4 shows the relationship between stretching stress and shrinkage. The shrinkage shows the strain which the amorphous part was subjected to under a shrinkage measurement temperature (100 and 110 °C). By increasing the stretching stress (decreasing the stretching temperature), better results in shrinkage property are obtained, especially low temperature shrink ability.

Figure 5 shows the relationship between stretching stress and tear strength. An increase in the stretching stress results in a higher tear strength. Figure 6 shows the relationship between the stretching stress and impact strength. Increasing the stretching stress results in a higher impact strength. This means that high stretching stress can obtain a good orientation. Figure 7 shows the relationship between stretching stress and Young's modulus. No effective trend can be observed. Figure 8 shows the relationship between stretching stress and haze. Again the haze keeps constant. The material has good clarity, and the pre-stretched film is cooled rapidly by cold water. Hence, the pre-stretched film also has good clarity. So the haze is not influenced very much by the stretching conditions.

In addition, both high and low stretching stress samples were taken in order to research the bubble deformation behaviour. These torques, inside bubble pressures and stretching stresses are shown in Table 3. The relationship between stretching torque and bubble shape is shown in Figure 9. The photographs show that an increase in the stretching torque, increases the bubble angle  $\theta$  in Figure 3. Figure 10 is a graph of these photographs calculated symmetrically and overlaid. Variations can be easily noted.

The necking phenomenon of the bubble is shown in Figure 11. The bubble deformation behaviour is shown in Figure 12, measured from the markings on the stretched bubble. This figure shows that by increasing the stretching torque (decreasing the temperature) a better stretch ratio uniformity is obtained. This stretch ratio dispersion occurs from the stretching start point, also called neck stretching, and begins the double bubble tubular film process. Therefore a lower stretching temperature (higher torque) is necessary to obtain a uniform thickness in the stretched film.

In addition, Figure 12 shows that the machine direction is stretched a little before starting to stretch in the transverse direction. This means that the double bubble tubular film process is not a perfect simultaneous biaxial stretching, but a partial sequential stretching. Too much pre-heat results in a greater sequential stretching. Figure 13 and Figure 14 shows bubble velocity and bubble strain rate during the double bubble tubular film process calculated from deformation length. This figure shows that as the stretching torque increases, the maximum bubble velocity and bubble strain rate are realized more quickly. The stretching stress and the maximum strain rate can be increased by decreasing the

stretching temperature.

### 3.2 Stretching by laboratory biaxial stretcher

The stretching stress and the properties of the films which are stretched by laboratory biaxial stretcher are shown in Table 4. These data show that the stretching stress of the films stretched by the laboratory biaxial stretcher is from about 2.5MPa to 15 MPa. Considering the double bubble tubular film process, the bubble is unstable under about 8 MPa stretching stress, which is shown in Table 2. This means that the appropriate stretching temperature range for the double bubble tubular film process is narrower than the tenter stretching process (laboratory biaxial stretcher) because of the bubble instability.

Figure 15 shows the relationship between the stretch ratio and the stretching force of each stretching temperature. And also, the relationship between the yield load and stretching force are shown. Therefore the most suitable stretching temperature in the double bubble tubular process is able to be predicted with relative accuracy. To be more precise in this case, the stretching temperature in the double bubble tubular process should be better under 116 °C at the least.

Figure 16 shows the relationship between stretching temperature and stretching stress, and is represented by a smooth quadratic curve. This means that the lower the temperature, the more the effect on the stretching stress. Further more, MD and TD display a similar curve, referring to only one of them is sufficient from now on.

Figure 17 shows the relationship between time and strain rate. This laboratory biaxial stretcher's strain rate is lower than the double bubble tubular film process shown in Figure 13.

Figure 18 shows the relationship between stretching temperature and shrinkage. A lower stretching temperature results in better shrinkage. This relationship is the same as the double bubble tubular film process, but shrinkage is less than the double bubble tubular film. This is because the film which is stretched by the laboratory biaxial stretcher is stretched isothermally, but the double bubble tubular film is stretched nonisothermally. In addition the laboratory biaxial stretcher's strain rate is lower than the comparative rate of the double bubble tubular film process.

Figure 19 shows the relationship between stretching temperature and tear strength. A lower stretching temperature has higher tear strength. Figure 20 shows the relationship between stretching temperature and Young's modulus, with no obvious trend noted.

Figure 21 shows the relationship between stretching temperature and haze. Between 110 °C and 116 °C no effective trend is displayed, however conditions become worse over 118 °C. It is recognized that film surface melt occurs over 118 °C, and when it is cooled the crystallinity increases, resulting in deteriorating film clarity. In the double bubble tubular film process, no haze samples could even be produced because of bubble instability.

The properties of the films which are stretched by the laboratory biaxial stretcher, show the same trends as those of the double bubble tubular film.

## 4. Conclusions

In the double bubble tubular film process, stretching temperature is a very important factor. A lower stretching temperature, increases the stretching stress, increases the bubble angle  $\theta$ , and increases the strain rate. As a result, shrinking properties and other physical properties become superior. Conversely increasing the stretching temperature decreases the stretching stress, and elongates the bubble shoulder, and also decreases the strain rate. As a result, shrink ability becomes worse and the physical properties are weaker. Also increasing the stretching temperature which decreases the stretching stress results in the beginning of the neck stretching, so film thickness tolerance deteriorates. Furthermore, stretch in the machine direction starts before stretch in the transverse direction. This means that the balance between the pre-heating temperature and stretch heating temperature is important in order to achieve a good balance of MD and TD properties.

In summary, bubble stability can be obtained by setting the stretching temperature as low as possible, while also keeping the stress levels low without rupturing the bubble, because this increases both the stretching strain rate and the stretching stress. There is a strong relationship between the stretching stress and the physical properties, and also between the stretching stress and the shrink ability of the stretched film. A higher stretching stress makes stronger physical properties and a better shrink ability. The relationship between the stretch ratio and the stretching force of the film, which is stretched by the laboratory biaxial stretcher, can be used for predicting the most suitable stretching temperature for the double bubble tubular film process. And film which is stretched by the laboratory biaxial stretcher shows the same property trends regarding the relationship between stretching stress (temperature) and properties, as does the double bubble tubular film process. So the biaxial stretcher's data can be used for predicting the trends of properties, according to stretching temperature for double bubble tubular film. But the laboratory biaxial stretching process has less stretching stress and a lower stretching strain rate than the double bubble tubular film process. In addition the film is stretched isothermally in the laboratory biaxial stretcher, but the double bubbler tubular film process is stretched nonisothermally. Henceforth the film which is stretched by the laboratory biaxial stretcher does not have as good a shrink ability as does double bubble tubular film.

## References

1. White, J.L., Film Processing p.412, Hanser (1999)
2. Takashige, M., and Kanai, T., Intern Polymer Processing V (1980) 4 p.287
3. Ree, S. and White, J.L., Intern Polymer Processing XVI(2001) p.272
4. Song, K., White J.L., Antec proceeding 57 p.1650 (1999)

5. Goldman, M. (Du Pont), U.S.Patent 2,979,777 (filed Nov.6 , 1958)
6. Blid, F., Robinson, W., (ICI), U.S.Patent 3,300,555 (filed Nov.12,1963)
7. Carl,A.,Lindstrom, Mass,A.,William.G.Baird,A.L.Bosse (W.R.Grace), U.S.Patent 3,260,776 (filed Oct.29,1964)
8. Tsuboshima, K., Kanho, T.,(Kojin) ,U.S.Patent 3,510549 (filed Apr.15,1969)
9. James,L.,Nash, Stanley,J.,Polich,(General Electric),U.S.Patent4,112,034 (filed May.5,1977)
10. Hayashi, K., Morihara, K., Nakamura, K.,(Chisso), U.S.Patent 4,279,580 (filed Dec.19,1979)
11. Schoenberg,Julian, H., (W.R.Grace) ,U.S.Patent 4,551,380 (filed May.10,1984)
12. Walter, B.,Mueller, (W.R.Grace), U.S.Patent 4,617,241 (filed Jan.23,1984)
13. Thomas, C.,Warren,(W.R.Grace),U.S.Patent 4,837,084 (filed Jul.2,1987)
14. David, A.,Harbourne, (Du Pont), U.S.Patent 4,226,905 (filed Apr.16,1979)
15. Stanley,Lusing, Nancy.M.,Mack, Jeffrey,M.,Schuetz,(Viskase), U.S.Patent 5,059,481 (filed Mar.28,1990)
16. Kanai, T., Tomikawa, M. , White, J.L. , Shimizu, J., Sen-i Gakkaishi 40[12], T-465(1984)
17. Kanai, T.,and Campbell ,G.A. , Film Processing 3.1, Hanser(1999)

Table 1 Properties of Linear Low Density Polyethylenes

	Unit	LLDPE-A	LLDPE-B	LLDPE-C	Testing method
Density	g/cm <sup>3</sup>	0.920	0.902	0.935	ASTM D 792
Melt Index	g/10min	1.0	1.0	2.5	ASTM D 1238
Melting point		121	100	124	DSC

Table 2 Production conditions and properties of the double bubble tubular films

			1	2	3	4	5
Materials			LL-A 70% LL-B 15% LL-C 15%				
Stretching ratio	-	MD×TD	5 X 5				
Ave. temp. of the pre-heaters		-	289	298	307	313	319
Ave. temp. of the stretching heaters		-	101	107	130	140	145
Film temperature after the pre-heater		-	107	112	116	120	127
Stretching torque	Nm	-	71.0 (broken)	52.2	44.9	38.4	31.2 (unstable)
Stretching force	N	-	676	497	428	366	297
Bubble inside pressure	Pa	-	-	0.53	0.43	0.37	-
Stretching stress <sub>MD</sub>	MPa	-	19.1	14.1	12.1	10.4	8.4
Stretching stress <sub>TD</sub>	MPa	-	-	13.2	10.8	9.2	-
Thickness	μ	-	15				
Tensile strength	MPa	MD/TD		134/172	140/162	133/150	
Elongation	%	MD/TD		143/130	130/140	140/140	
Young's modulus	MPa	MD/TD		301/353	324/318	304/340	
Tear strength	mN	MD/TD		176/127	137/118	118/118	
Impact strength	J	-		0.81	0.72	0.63	
Haze	%	-		1.2	1.4	1.3	
Shrinkage MD/TD	%	90		13/15	13/15	12/14	
		100		23/29	23/26	20/24	
		110		46/50	44/48	44/47	
		120		74/74	74/72	72/72	

Table 3 Stretching torque, inside bubble pressure and stretching stress of measuring the bubble deformation behaviour samples

	Unit	1	2
Stretching torque	Nm	58.7	35.5
Inside bubble pressure	Pa	0.56	0.34
Stretching stress <sub>MD</sub>	MPa	15.8	9.6
Stretching stress <sub>TD</sub>	MPa	14.0	8.5

Table 4 Properties of the films stretched by laboratory biaxial stretcher

			1	2	3	4	5	6	7	8	9
Materials			LL-A 70% LL-B 15% LL-C 15%								
Stretching temperature		-	108 broken	110	112	114	116	118	120	122	124 melt
Stretching force (Str. ratio=5)	N	MD TD		64.1 64.5	52.1 53.3	40.0 42.8	31.4 34.9	22.1 28.9	14.7 18.4	9.8 11.8	
Stretching stress	MPa	MD TD		15.3 15.4	12.4 12.7	9.52 10.2	7.47 8.31	5.25 6.88	3.50 4.39	2.33 2.80	
Thickness	μ	-	12								
Tear strength	mN	MD TD		-	255 353	235 176	157 137	118 137	137 137	137 137	
Haze	%	-		0.8	0.8	0.9	0.9	1.1	1.7	2.7	
Young's modulus	MPa	MD TD		270 299	293 284	275 296	283 312	281 295	269 275	293 281	
Shrinkage MD/TD	%			9/9 15/16 43/43 73/70	8/8 19/20 37/38 71/69	7/7 15/16 33/34 73/70	7/7 12/13 29/30 70/68	5/6 10/11 26/27 65/63	4/4 9/10 16/17 55/57	2/2 6/6 13/13 45/39	

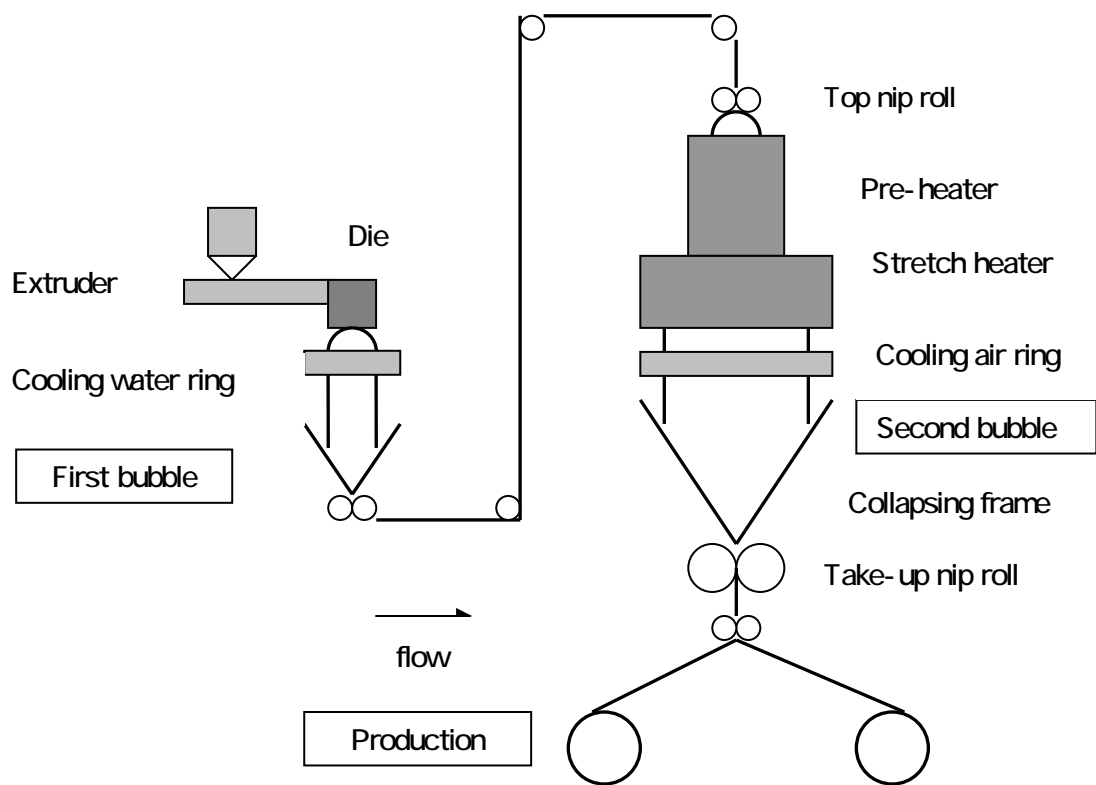


Figure 1 Schematic drawing of double bubble tubular film blowing apparatus

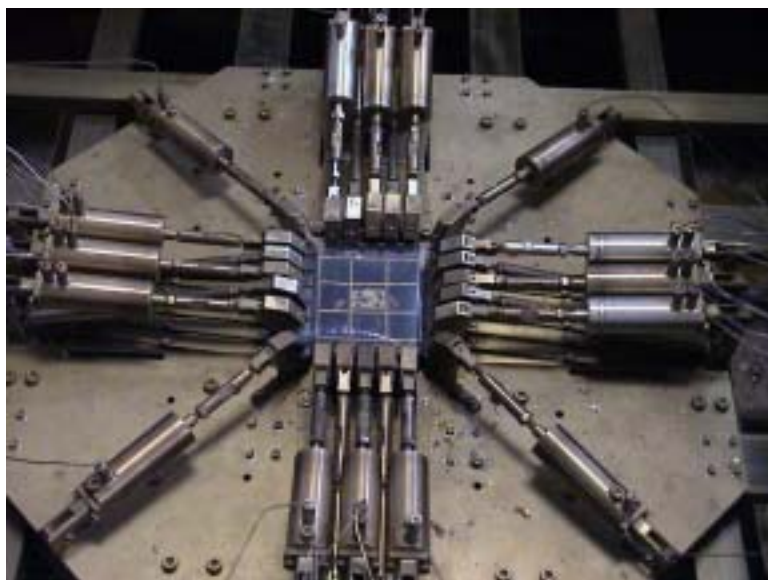


Figure 2 Laboratory biaxial stretcher



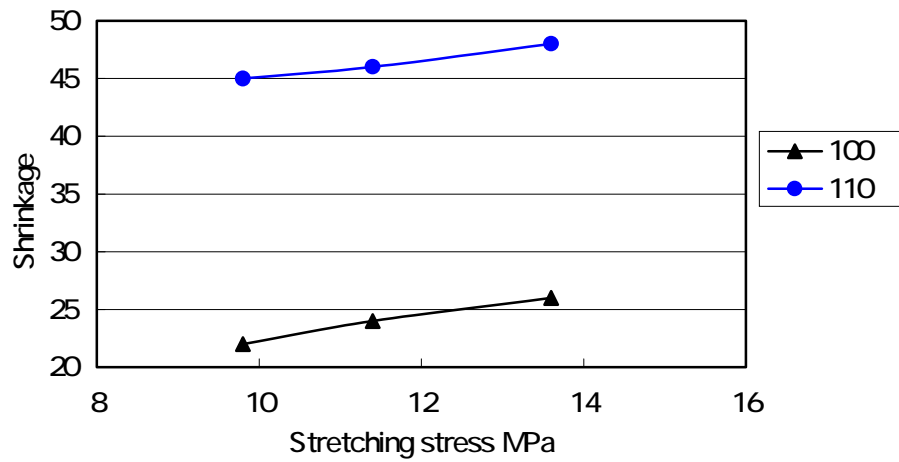


Figure 4 Relationship between stretching stress and shrinkage

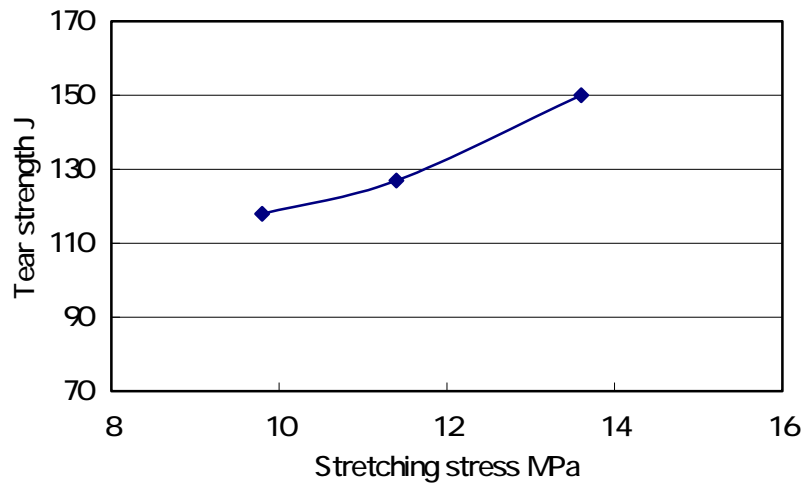


Figure 5 Relationship between stretching stress and tear strength

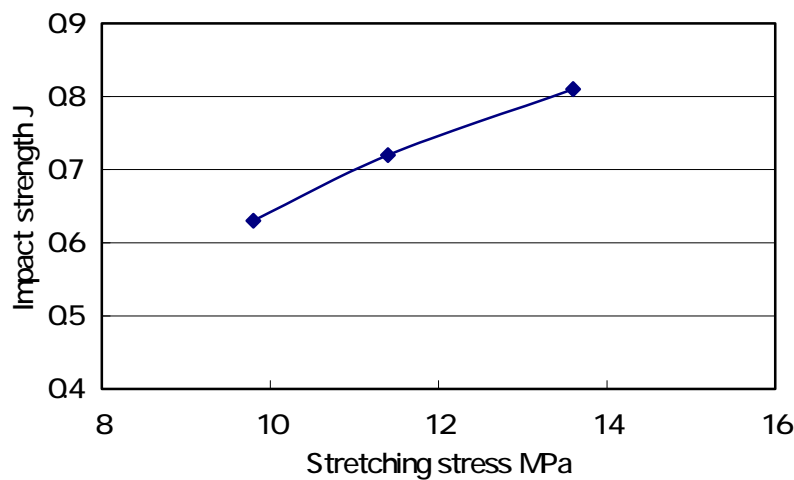


Figure 6 Relationship between stretching stress and impact strength

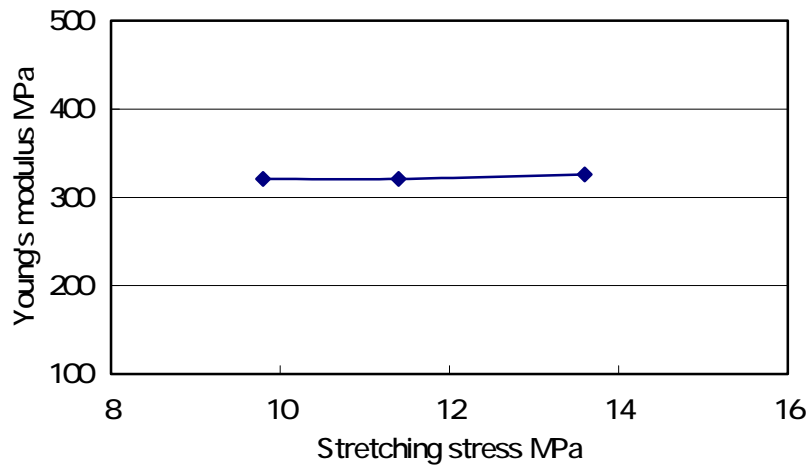


Figure 7 Relationship between stretching stress and Young's modulus

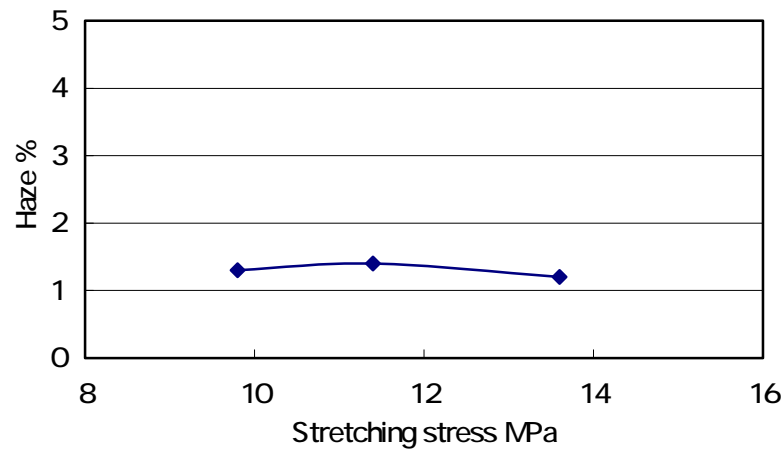


Figure 8 Relationship between stretching stress and haze



Torque=58.7Nm



Torque=35.5Nm

Figure 9 Photograph of bubble shape

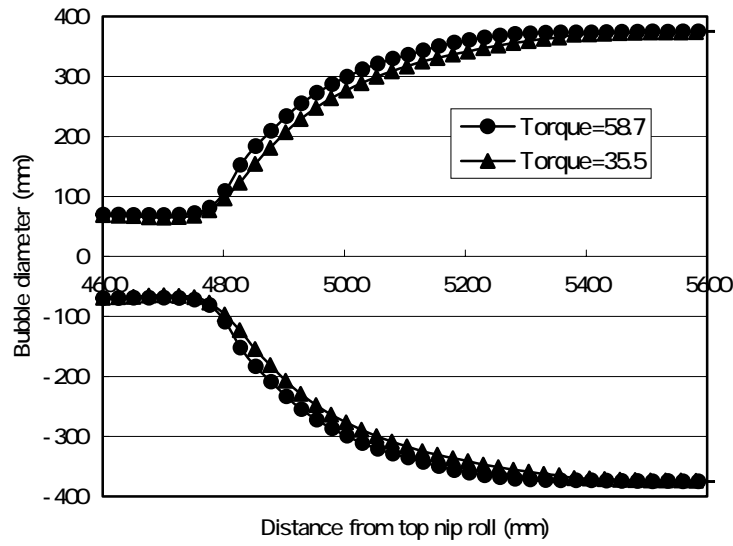


Figure 10 Relationship between stretching torque and bubble shape

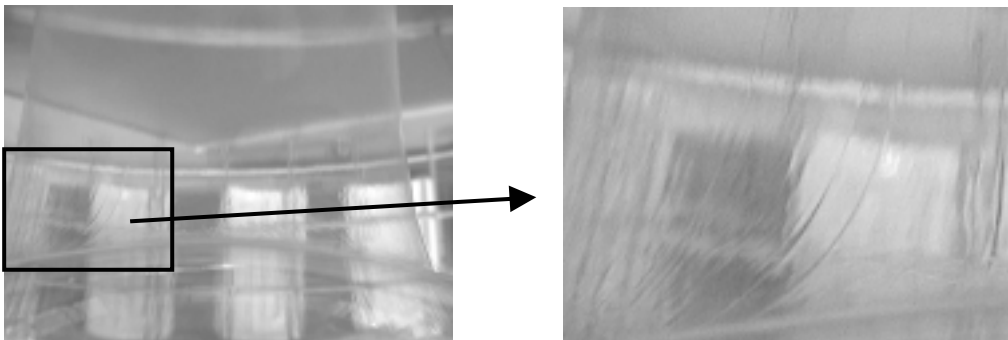


Figure 11 Necking phenomenon of double bubble tubular film process

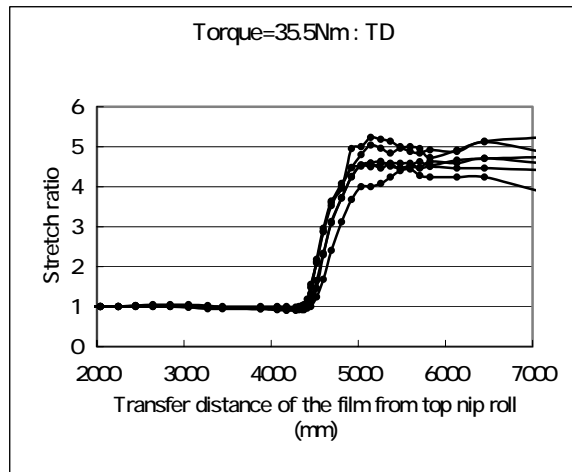
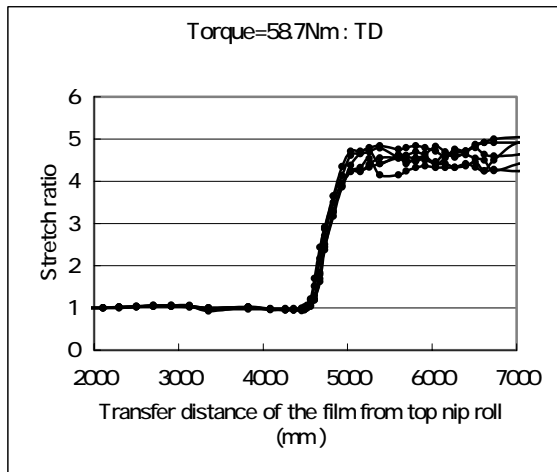
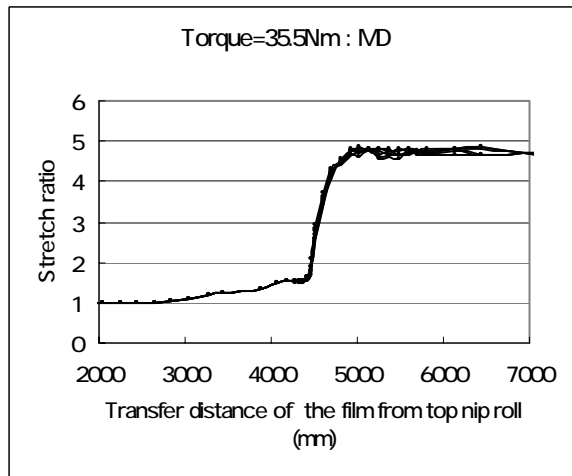
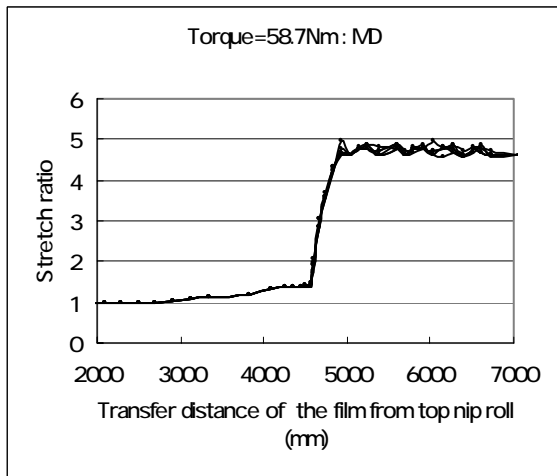


Figure 12 Bubble deformation behaviour of the double bubble tubular process

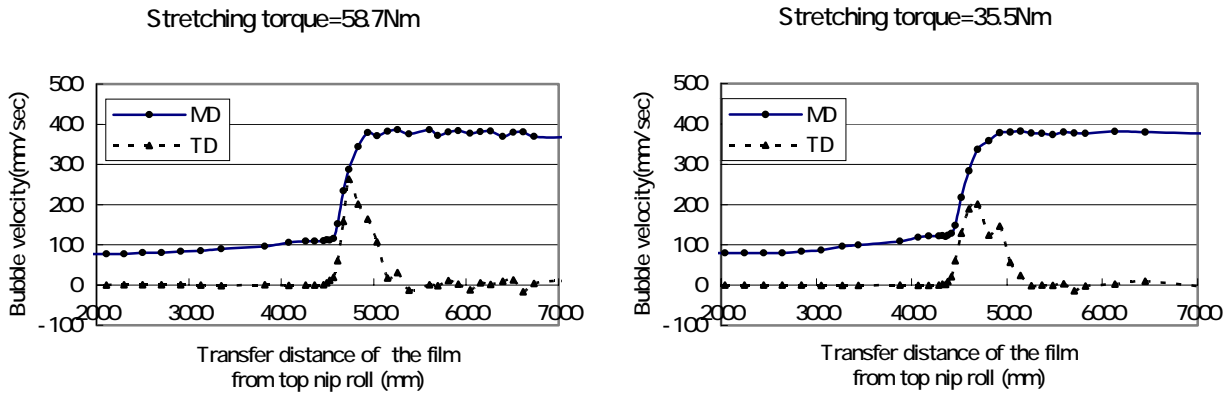


Figure 13 Bubble velocity of the double bubble tubular process

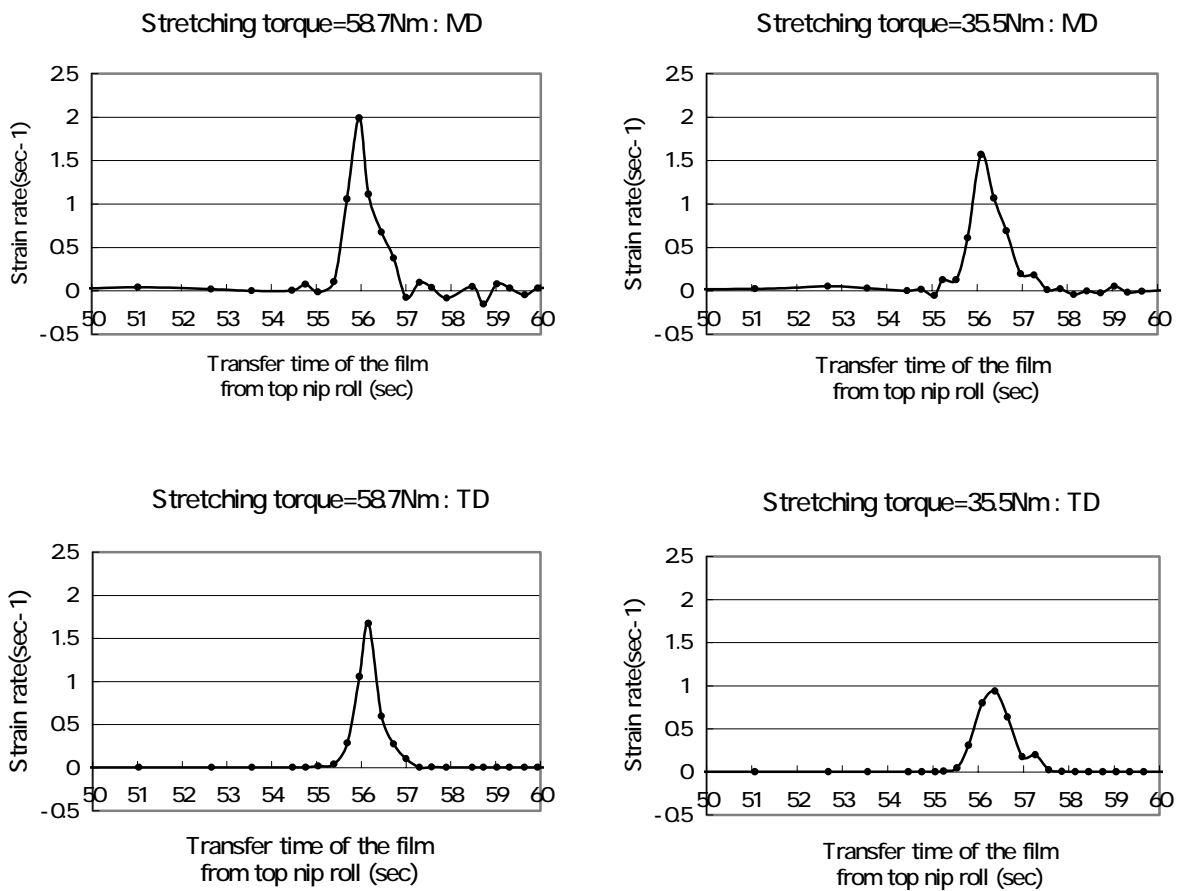


Figure 14 Bubble strain rate of the double bubble tubular process

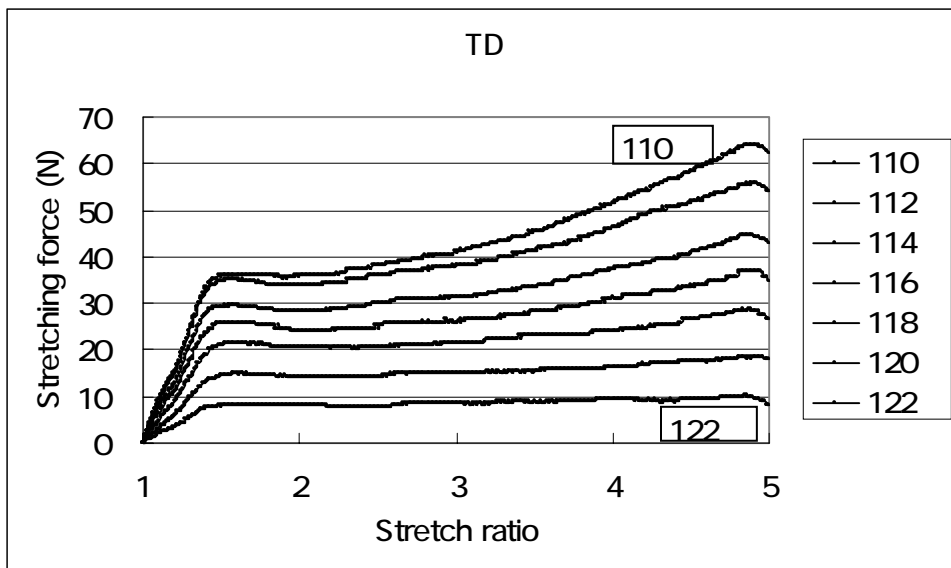
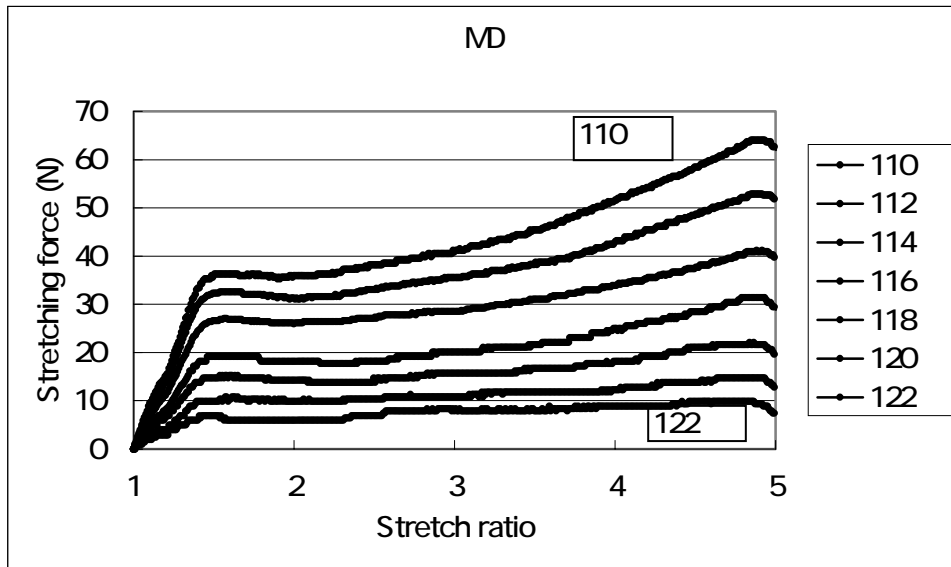


Figure 15 Relationship between stretch ratio and stretching force

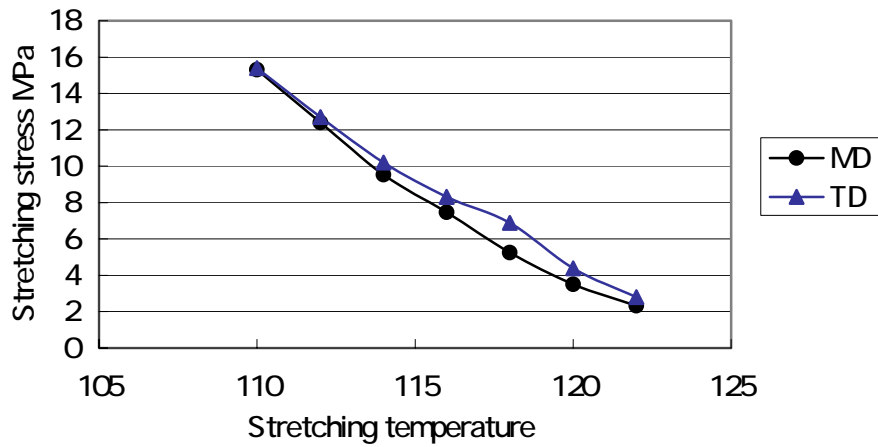


Figure 16 Relationship between stretching temperature and stretching stress of the films which are stretched by laboratory biaxial stretcher

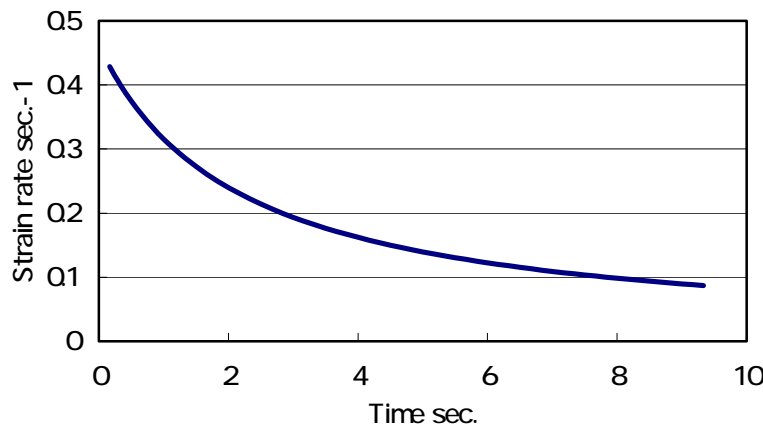


Figure 17 Strain rate of laboratory biaxial stretcher

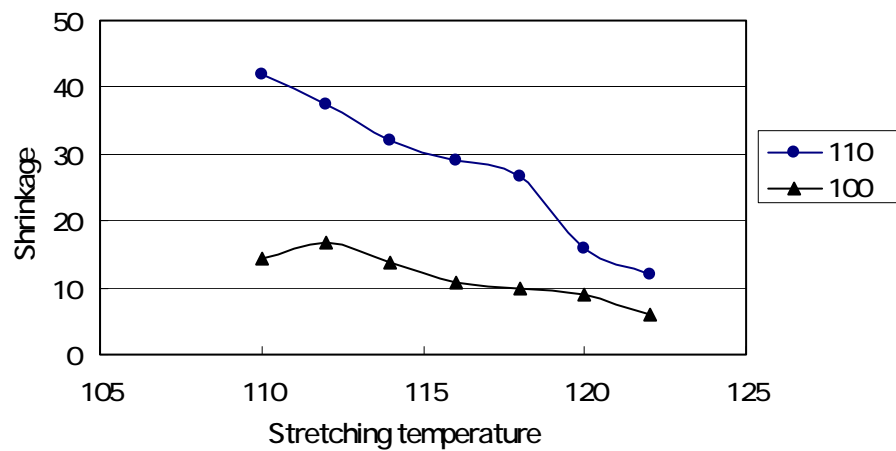


Figure 18 Relationship between stretching temperature and shrinkage of the films which are stretched by laboratory biaxial stretcher

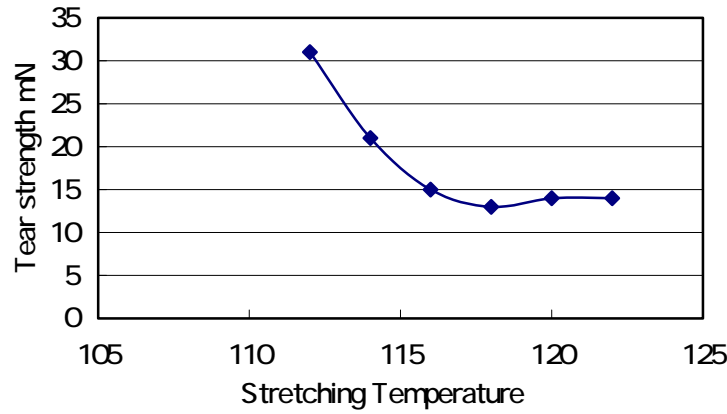


Figure 19 Relationship between stretching temperature and tear strength of the films which are stretched by laboratory biaxial stretcher

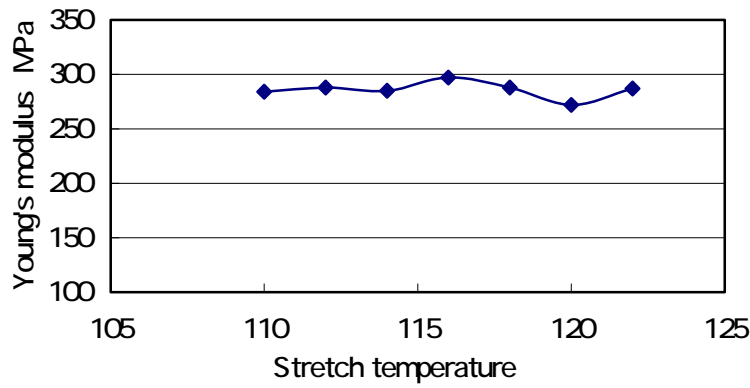


Figure 20 Relationship between stretching temperature and young's modulus of the films which are stretched by laboratory biaxial stretcher

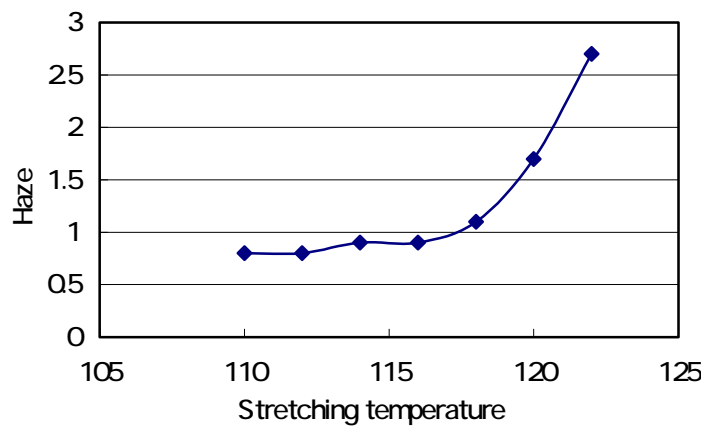


Figure 21 Relationship between stretching temperature and haze of the films which are stretched by laboratory biaxial stretcher





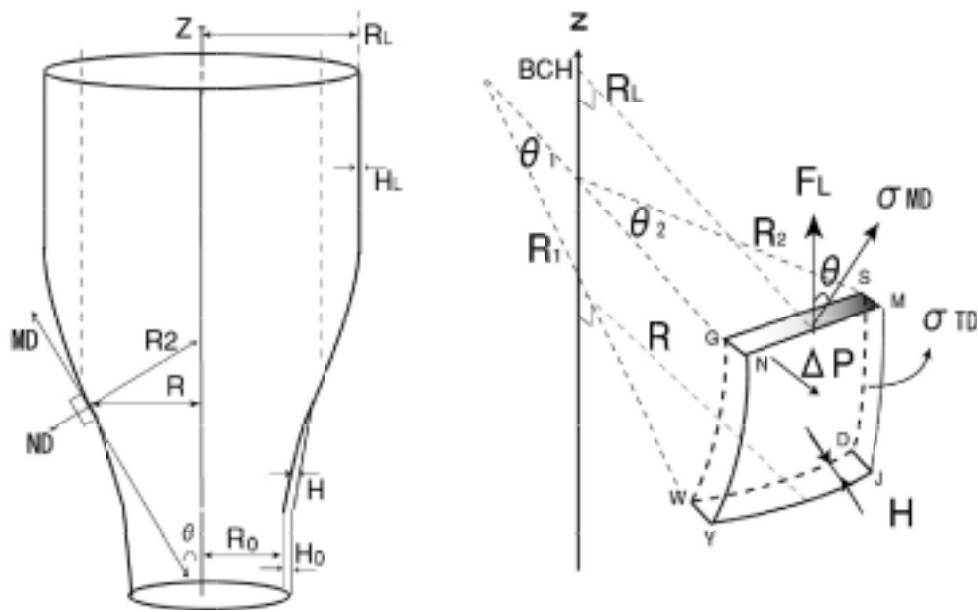


Figure 3 Schematic diagram of force balance on the bubble